VIII-II-1. Project Research

Project 1

PR1 Project Research on Study of Microstructural Evolution and Physicality Changes in Irradiated Solid Materials

Q. Xu

Research Reactor Institute, Kyoto University

OBJECTIVES: Macroscopic properties of materials, such as mechanical property, optical property, electrical property, are changed by the irradiation with high energy particles. In order to investigate the mechanism of macroscopic property changes in irradiated materials, irradiations of high energy particles, such as fission neutrons, ions, electrons and γ rays have been carried out for several decades years. However, the processes of defect production, defect reaction and defect cluster formation are still not fully understood. The same number of interstitials and vacancies are formed by displacement damage under high energy particle irradiation of crystalline materials. If the two kinds of point defects behave symmetrically, significant microstructural development by irradiation damage would not be expected. Without exception, the development starts and proceeds only when the balance between interstitials and vacancies is broken for some reasons. In fact, there are great varieties of sources of asymmetry in the irradiated materials. Therefore, it is important to understand the mechanism producing each source of asymmetry to clarify the damage structural development.

To perform these studies, irradiation experiments using various kinds of high energy particles at wide range of irradiation conditions are necessary. In the Research Reactor Institute, there exist irradiation fields of neutrons, ions, electrons and γ rays from low to high temperatures.

RESULTS: The allotted research subject (ARS) and the name of co-researches in each ARS are listed below. A number of important data were already obtained. Details are presented in this progress reports.

ARS-1

Thermally stimulated current studies on electron irradiated ZnO bulk single crystals

(K. Kuriyama, Y. Suzuki, Y. Izawa, K. Kushida, and Q. Xu)

ARS-2

Fabrication and observation of nano-cell structure on compound semiconductor

(M. Taniwaki and N. Nitta)

ARS-3

Study on formation and recovery of damage in irradiated crystalline materials

(A. Kinomura, Y. Nakano, Q. Xu and T. Yoshiie)

ARS-4

Optical vibronic emission spectra for F_2 type centers in neutron irradiated α-Al_2O_3

(Rahman Abu Zayed Mohammad Saliqur, A. Sidike, T. Awata, Q. Xu, K. Atobe and N. Yamashida)

ARS-5

Positron annihilation lifetime compared with thermal diffusivity in ceramics irradiated by 30MeV electron using KURRI-LINAC

(M. Akiyoshi, I. Takagi, T. Yoshiie, Q. Xu and K. Sato)

ARS-6

Vacancy type defect in Cu-Cr-Zr alloy induced by 28 MeV electron irradiation at 77K studied by positron annihilation

(Y. Nagai, T. Toyama, M. Hatakeyama, A. Kuramoto, H. Takamizawa, T. Yoshiie, Q. Xu)

ARS-7

Defects study for bulk glassy alloys damaged by electron irradiations

(F. Hori, Y. Fukumoto, A. Ishii, A. Iwase, Q.Xu and T.Yoshiie)

ARS-8

Microstructure of neutron irradiated vanadium alloys in a liquid sodium environment

(K. Fukumoto, M. Iwasaki and Q. Xu)

ARS-9

Damage evolution in neutron-irradiated metals during neutron irradiation at elevated temperatures

(I. Mukouda, K. Yamakawa, T. Yoshiie , Q. Xu)

ARS-10

Effects of thermal aging on positron annihilation behaviors of ODS and non-ODS ferritic steels

(R. Kasada, S.H. Noh, J.H. Lee, A. Kimura, K. Sato Q. Xu and T. Yoshiie)

ARS-11

Interaction between radiation defects and hydrogen studied by positron annihilation spectroscopy

(H. Tsuchida, H. Tanaka, A. Itoh, T. Yoshiie and Q. Xu)

ARS-12

Austenitic stainless steel irradiated with high-energy particle at high temperature

(K. Sato, X.Z. Cao, Q. Xu and T. Yoshiie)

ARS-13

Mechanical properties of tungsten at high temperature

(K. Tokunaga, K. Araki, T. Fujiwara, Y. Miyamoto, Q. Xu and T. Yoshiie)

採択課題番号 21P1　固体材料の照射による微細組織及び物性変化の解明　プロジェクト
（京大・原子炉）徐　虬

PR1-1 Thermally Stimulated Current Studies on Electron Irradiated ZnO Bulk Single Crystals

K. Kuriyama, Y. Suzuki, Y. Izawa, K. Kushida[1] and Q. Xu[2]

College of Engineering and Research Center of Ion Beam Technology, Hosei University
[1]Osaka kyoiku University
[2]Research Reactor Institute, Kyoto University

INTRODUCTION: In order to confirm the theoretical calculations [1] of the native defects, several experiments on single crystal ZnO have been performed using deep-level-transient spectroscopy (DLTS) and thermally stimulated current (TSC) studies [2]. In the present study, we study the electron-irradiated induced defect in ZnO by the TSC method with excitation near the energy band gap using a blue light emitting diode (LED).

EXPERIMENTS: The ZnO single crystals used here were grown at Tokyo Denpa Co., Ltd. using the hydrothermal method. The dimensions of the c face cut-samples were 5 x 5 x 0.5 mm^3. A 30 MeV electron irradiation was performed at room temperature with a beam current 18 $\mu A/cm^2$ using an electron linear accelerator facility at Kyoto University Research Institute. The irradiation dose was 7.8 x 10^{17} e^-/cm^2.

RESULTS: Figure 1 (a) shows the TSC spectrum of electron-irradiated ZnO taken after the excitation with the blue LED. This spectrum is normalized with a relation of [I(TSC)-I(dark)]/I(PC(90 K)), where I(TSC) is TS current, I(dark) the dark current, and I(PC) the photocurrent at 90 K. Two broad TSC spectra were observed at a temperature ranging from 90 to 300 K. The curve fitting toolbox of MATLAB (The Math Works. Inc.) was used to resolve the broad spectrum to optimum Gaussian curves as done in our previous work [2]. Using the toolbox, the broad spectrum is resolve to six traps, P_1(T_m = 90 K), P_2(140 K), P_3(160 K), P_4(194 K), P_5(257 K), and P_6(297 K). According to the approximate relationship [3] $E_i \approx kT_m\ ln(T_m^4/\beta)$, where E_i is the ionization energy (trap depth), k Bolzmann's constant, T_m the TSC peak temperature, and β the heating rate for the thermal scan (a typical value used here: 0.14 Ks^{-1}), the ionization energies for these traps were calculated as $E_i(P_1)$ = 156, $E_i(P_2)$ = 258, $E_i(P_3)$ = 302, $E_i(P_4)$ = 381, $E_i(P_5)$ = 545, and $E_i(P_6)$ = 664 meV. E_i values estimated by the present TSC study contain an uncertainty of ±20 meV. The ionization energies for P_1-P_4 traps are coincident with those of the un-irradiated ZnO wafer (figure 1(b)) as reported previously [2]. We noticed that two new peaks, P_5 and P_6, appeared after electron-irradiation. Although the TSC method usually cannot distinguish the sign of a trap (an electron or a hole trap), possible origins of the observed traps are discussed below. According to the calculations [1], the P_5 trap may be related to the energy level located at 510 meV above the valence band, which is a deep acceptor transition level, ε(-/2-) of Zn vacancy. Recent TSC study [4] suggests that an electron-irradiation induced defect with an activation energy of 150 meV may be related to a deep acceptor transition level, ε(0/-), of Zn vacancy. Another new trap, P_6, may be related to an energy level located at 700 meV (or 570 meV [4]) above the valence band, which is a deep acceptor transition level, ε(0/-), of oxygen interstitial. Considering the errors inherent in the local density approximation (LDA), P_5 and P_6 traps observed after electron-irradiation are tentatively assigned to the zinc vacancy and interstitial oxygen, respectively. Because, it has been reported that electron-irradiation introduces not only an oxygen vacancy but also zinc vacancy [4]. Furthermore, the electron-irradiation will induce both an oxygen vacancy and interstitial oxygen, namely Frenkel type defects. And also, it has been pointed out that the green emission in ZnO consists of the oxygen and zinc vacancies. Therefore, it would be reasonable to assign two traps, P_5 and P_6, to zinc vacancy and interstitial oxygen, respectively.

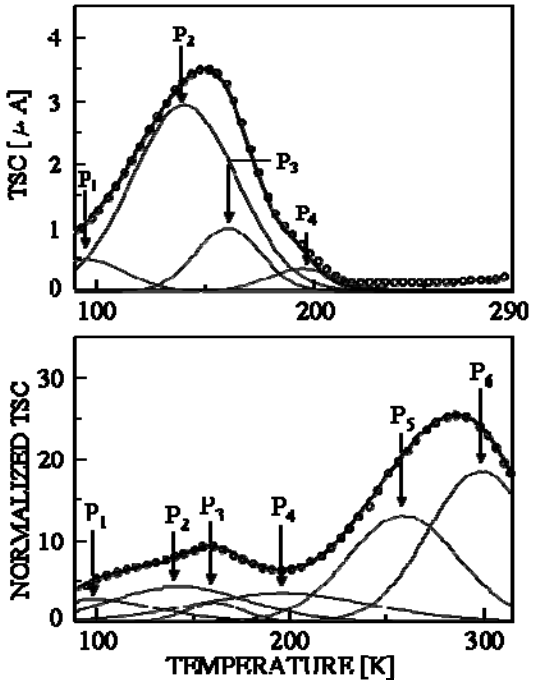

Fig. 1. (a) A typical normalized TSC spectrum {i.e., [I(TSC) -I(dark)]/I(PC(90 K))},for illumination with a blue LED in electron irradiated single crystal ZnO. The TSC spectrum is resolved to six traps. (b) TSC spectra resolved to four traps inunirradiated single crystal ZnO.

REFERENCES:

[1] A. Janotti, C.G.van de Walle, J. Cryst. Growth.,**287** (2006) 58.
[2] K. Kuriyama, M. Ooi, K. Matsumoto, K. Kushida, Appl. Phys. Lett., **89** (2006) 242113.
[3] D.C. Look, Semicond. Semimet., **19** (1983) 75.
[4] Z.-Q. Fang, B. Claflin, D.C. Look, G.C. Farlow, J. Appl. Phys.,**101** (2007) 086106.

採択課題番号 21P1-1　化合物半導体の照射効果と電気的・光学的特性に関する研究　プロジェクト
（法政大・工）栗山一男（法政大院）鈴木優平、井澤佑介　（大阪教育大）串田一雅
（京大・原子炉）徐 虬

PR1-2 **Fabrication and Observation of Nano-Cell Structure on Compound Semiconductor**

M. Taniwaki[1] and N. Nitta[2]

[1]*Department of Environmental Systems Engineering, Kochi University of Technology*
[2]*Department of Mechanical Engineering, Kobe University*

Many point defects are induced in ion irradiated materials. Some of the induced vacancies are not annihilated and gather self-organizationally to create cellular structure in GaSb, InSb and Ge [1-5]. The new nano-fabrication on the basis of this knowledge consists of two procedures, in order to realize the ordered two dimensional nano-cell lattices [6]. The first process (top-down) is to produce an ordered initial structure of voids or hollows artificially and the second (bottom-up) is to develop it into nano-cell cell lattice self-organizationally without disturbing the regularity. The second procedure to create many vacancies and interstitials developing voids or hollows is performed by particle irradiation, usually ion irradiation. The first procedure is possible to be performed by means of lithography as conventional top-down process technique and also possible by well-controlled ion irradiation. The authors chose the ion irradiation due to the following reasons. First it is able to create both of voids and hollows by ion irradiation, though lithography cannot induce the voids under the surface. Second, both processes of top-down and bottom-up can be carried out without transportation of the samples by using FIB apparatus (focused ion beam). Moreover we can observe high resolution SIMS image of fabricated surface structure in FIB simultaneously, which enable the easy evolution of this new nano-technology [7].

GaSb and InSb single crystal wafers were used in this work. Initial structures (closed packed lattices of voids) were fabricated on the wafers by irradiation of Ga^+ beam with 5 nm diameter and the initial structures were developed by repetition of image scanning mode of FIB at room temperature. The variable parameters were acceleration voltage, ion dose per one lattice point and the lattice constant (neighboring void (or hollow) distance). The SIMS image was recorded simultaneously with fabrication of the initial structure and each image scanning.

The close packed voids lattice was fabricated on GaSb and its change by image scanning in FIB. An initial void was formed by irradiation of 1.12×10^4 Ga^+ and the dose per one image scanning was 1.46×10^{15} ions/cm^2. The invisible voids in the initial pattern became visible hollows as their top surfaces are removed by the scanning, and voids are newly formed in the region where the initial structure was not created, and these voids grew with increasing scan times. The shape of the initial voids changed from round shape into hexagon by further scanning, when the thickness of partitioning walls was almost constant, which was estimated to be 15 nm from FIB image. The regularity of the cell lattice increased by irradiation, however many times scanning disturbs the cell lattice and the regularity is severely lost. The cell diameter increases and the partitioning wall thickness decreases and saturates. Though the ion irradiation develops the cell structure initially, heavy irradiation disturbs the regularity. The most ordered nano-cell lattice was obtained at the 30 keV Ga^+ dose of 7.3 – 8.8 x 10^5 ions/cm^2. In this experiment using a close-packed nano-cell lattice, the formation of the secondary voids was certainly depressed in the initial structure created region which differ much from the results using tetragonal lattice.

REFERENCES:

[1] N. Nitta, M. Taniwaki, T. Suzuki, Y. Hayashi, Y. Satoh and T. Yoshiie: J. Jpn. Inst. Met., **64**(2000)1141(in Japanese).

[2] N. Nitta, M. Taniwaki, T. Suzuki, Y. Hayashi, Y. Satoh and T. Yoshiie, Mater. Trans., **43**(2002) 674.

[3] N. Nitta, M. Taniwaki, Y. Hayashi and T. Yoshiie, Physica, B **376-377**(2006)881.

[4] N. Nitta, Y. Ohoka, K. Satoh, Q. Xu, Y. Hayashi, T. Yoshiie and M. Taniwaki, Mater. Trans. **49** (2008) 1546.

[5] N. Nitta, M. Taniwaki, Y. Hayashi and T. Yoshiie, J. Appl. Phys., **92**(2002)1799.

[6] N. Nitta and M. Taniwaki, Nucl. Instum. Methods. Phys. Res., B **206** (2003) 482.

[7] N. Nitta and M. Taniwaki, Physica B, **376-377** (2006)872-876.

採択課題番号21P1-2　化合物半導体イオン照射挙動　プロジェクト
（高知工科大・物質･環境）谷脇雅文, Dang Thai Giang　（神戸大・機械）新田紀子, 長谷川季也
（京大・原子炉）義家敏正, 林禎彦

PR1-3 Study on Formation and Recovery of Damage in Irradiated Crystalline Materials

A. Kinomura, Y. Nakano[1], Y. Hayashi[1], Q. Xu[1] and T. Yoshiie[1]

National Institute of Advanced Industrial Science and Technology (AIST)
[1] *Kyoto University Research Reactor Institute (KURRI)*

INTRODUCTION: The effects of ion irradiation damage have been extensively studied for various materials. However, it should be noted that residual defects experimentally detected are often less than primary defects theoretically calculated, implying that both damaging and recovery processes coexist during irradiation. A typical case of the recovery effect is the ion beam induced epitaxial crystallization in Si, where implantation-induced amorphous layers are epitaxially recrystallized under ion beam irradiation at elevated temperatures. It is important to investigate such competing processes for the application and fundamental studies on interactions of energetic particles (ions and neutrons) with materials. This study aims to investigate the radiation effects in ion-irradiated crystalline materials.

EXPERIMENTS: Two types of experiments were performed in this study: (1) Recovery of ion-implantation induced damage by neutron irradiation in single crystalline Si; (2) Damage introduction under ion irradiation in pure metals for characterization of ion-induced damage. In the first experiment, radiation damage was introduced in single crystalline Si by self-ion (Si) irradiation, followed by neutron irradiation in the Material Controlled Irradiation Facility (Irradiation temperature $\geq$200 ºC) or in the Core Irradiation Facility (Irradiation temperature ~90 ºC) at KURRI. The irradiated/annealed samples were characterized by Rutherford backscattering/channeling (RBS/C). In the second experiment, mirror-polished pure (99.99%) Fe and Ni substrates were implanted with 150 keV Ar ions at room temperature or elevated temperatures (300 – 500 °C). For comparison, self-ion implantation was performed by the heavy-ion accelerator at KURRI. Irradiated metals were analyzed by positron annihilation spectroscopy (Doppler broadening and lifetime measurements).

RESULTS: In the experiment on neutron-induced damage recovery, it is necessary to compare the Si-implanted samples thermally annealed for the same time as the neutron irradiation. The thermal annealing corresponding to the core-irradiation samples is in preparation. In the experiment on the ion-induced damage in pure metals, Ni and Fe samples have been irradiated with 60 keV Ni or Fe ions to investigate the chemical effects of ions on damage. Table 1 shows the ion species and their beam current obtained by the heavy-ion accelerator at KURRI for this experiment. Sufficient beam current for our experiment was obtained with both Ni and Fe ions. Besides, the Ar ion irradiation can be performed with ion flux (beam current) similar to those of metal ion beams. Fig. 1 shows the positron lifetimes from the Ni-irradiated samples. The measured lifetime spectra were decomposed into two lifetime components, where the shorter and longer lifetimes correspond to lifetimes from metals and Kapton, respectively. The Kapton sheet was used to cover unirradiated regions of the samples. A similar trend was observed between the Ni and Ar irradiations. A difference between two ions is ascribed to different projected ranges of Ni (0.18 μm) and Ar (0.24 μm). The chemical effects of implanted Ar ions may be negligible. Fe-irradiated Fe samples were prepared and we plan to measure positron lifetimes of them in the same way as the Ni irradiated sample.

ACKNOWLEDGMENT: We would like to thank colleagues in AIST for their assistance on this study.

Table 1. Ion species and beam current obtained by the heavy-ion accelerator at KURRI.

Ion	Ni^+	Fe^+	Ar^+
Source material	Pure Ni	Pure Fe	Sputtering gas
Energy (keV)	60	60	60
Current (μA)	0.26	0.18	0.2 - 8

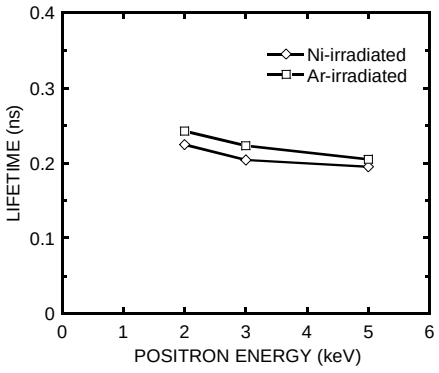

Fig. 1. Positron lifetime as a function of energy for the Ni- and Ar-irradiated Ni samples.

採択課題番号 21P1-3　照射下の結晶材料における損傷形成と回復過程の研究　プロジェクト
（産総研）木野村淳（京大・原子炉）中野幸廣、林　禎彦、徐　虬　、義家敏正

PR1-4 Photoluminescence Properties of Natural Na_2SO_4 Activated with Rare Earth Ions

Rahman Abu Zayed Mohammad Saliqur, Aierken Sidike[1], T. Awata[2], Q. Xu[3], K. Atobe and N. Yamashita

Okayama University
[1] *Xinjiang Normal University*
[2] *Naruto University of Education0*
[3] *Reactor Research Institute, Kyoto University*

INTRODUCTION: Thenardite (Na_2SO_4) is a fluorescent mineral showing white luminescence under short-wave ultraviolet (UV) light (253.7 nm Hg line), milk-white luminescence under long-wave UV light (365.0 nm Hg line), and long phosphorescence. The contents of trace elements in natural thenardite from Ai-Ding Salt Lake at Turpan, Xinjiang, China, were determined using an inductively coupled plasma-mass spectrometry (ICP-MS) analyzer [1]. It was found that the thenardite from Ai-Ding Salt Lake consists of extremely pure Na_2SO_4. The objectives of this study are to prepare Na_2SO_4:Eu and Na_2SO_4:Sm phosphors by activating natural thenardite with Eu and Sm, respectively and to obtain the PL and excitation spectra of as-prepared and γ-ray-irradiated phosphors.

EXPERIMENTS: Natural thenardites from Ai-Ding Salt Lake were obtained from collections of the Xinjiang Geology and Mineral Museum, China. Small amounts of EuF_3 and SmF_3 were mixed with powered thenardite and heated at 900° and 920°C respectively for 20 min in air. A few Eu and Sm-doped thenardite samples were exposed to γ-rays of 2–98 kGy at ambient temperature using the ^{60}Co γ-ray irradiation source of the Kyoto University Reactor.

RESULS and DISCUSSIONS: The relative efficiency of the Eu^{2+} Luminescence of the γ-ray-irradiated phosphor at the exposure of 46 kGy increased up to 3.0 times that of the non-irradiated phosphor. The features of the Eu^{2+} band in the PL spectra were not changed by γ-ray irradiation. Figure 1 shows relative PL intensities of the Eu^{2+} and Eu^{3+} bands of non-irradiated and γ-ray-irradiated Na_2SO_4:Eu as a function of γ-ray exposure. With an increase in the γ-ray exposure, the PL intensities of the Eu^{2+} band (*open circles*) increased, whereas those of the Eu^{3+} band (*filled circles*) decreased. The enhancement of the luminescence efficiency of the Eu^{2+} band upon γ-ray irradiation can be ascribed to the conversion of Eu^{3+} to Eu^{2+} in Na_2SO_4.

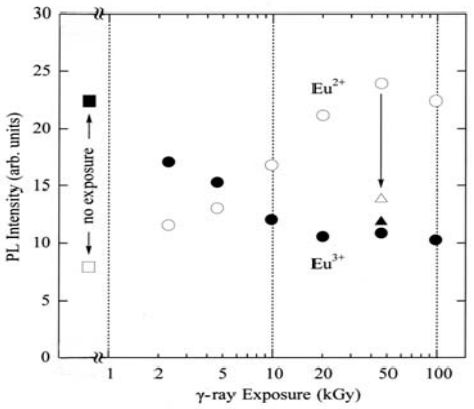

Fig. 1. Relative PL intensities of Eu^{2+} band (*open square, circles and triangle*) and Eu^{3+} band (*filled square, circles and triangle*) of non-irradiated(*squares*) and γ-ray-irradiated (*circles and triangle*) thenardite Na_2SO_4:Eu as a function of γ-ray exposure (kGy).

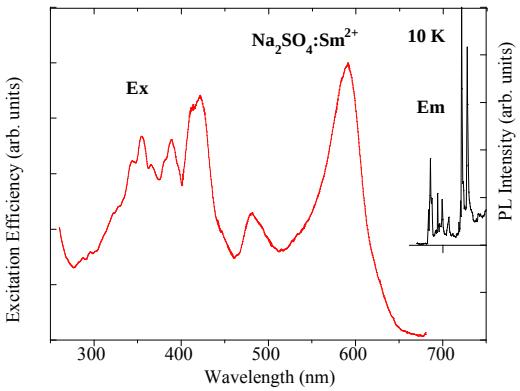

Fig. 2. Optical excitation spectrum (left) and PL spectrum of γ-ray irradiated natural Na_2SO_4. Excitation spectrum was obtained by monitoring the emission at 729 nm, and PL spectrum was obtained under 590-nm excitation. Both the measurements were done at 10 K.

Figure 2 shows the excitation and emission spectra of Sm^{2+} in γ-ray irradiated Na_2SO_4:Sm which was not observed in non-irradiated phosphors. It might happen due to conversion of some Sm^{3+} centers into Sm^{2+} centers caused by γ-ray irradiation in the Na_2SO_4 crystals.

REFERENCES:

[1] Aierken Sidike, Keyoumu Niyazi, H.-J. Zhu, K. Atobe, N. Yamashita, Phys. Chem. Miner., **36** (2009)119-124.

採択課題番号 21P1−4　放射線照射による高融点化合物の欠陥生成と誘起発光過程　プロジェクト（鳴教大）粟田高明，大島康介，前田偉志，藤原隆明（岡大・教育）跡部紘三，山本駿，安藤尚記（岡大・自然科学）ラハマン・アブ・ジャイド　（京大炉）義家敏正，徐虫し

PR1-5 Positron Annihilation Lifetime Compared with Thermal Diffusivity in Ceramics Irradiated by 30MeV Electron Using KURRI-LINAC

M. Akiyoshi[1], I. Takagi[1], T. Yoshiie[2], Q. Xu[2] and K. Sato[2]

[1]*Faculty of Engineering, Kyoto University*
[2]*Research Reactor Institute, Kyoto University*

INTRODUCTION:

Thermal diffusivity is one of the most important factors for ceramic materials expected to be used in fusion reactor blanket or divertor. In these ceramic materials, unlike metals, heat is mainly carried by phonon, and phonon is scattered by irradiation-induced defects to show severe degradation in thermal diffusivity after neutron irradiation [1-3].

In the previous work (KUR Progress Report 2007), positron annihilation lifetime of the specimens irradiated by 30MeV electron was measured and the spectrum was compared with that of unirradiated specimen. In this work, positron annihilation lifetime was analyzed and the average lifetime was compared with thermal diffusivity.

EXPERIMENTS:

Typical structural ceramics (α-Al_2O_3, AlN, β−Si_3N_4 and β-SiC) were irradiated by 30MeV electron using the KURRI-LINAC up to 1.5×10^{24}e/m^2 (correspond to 0.01dpa) at 300K in the water-cooled specimen holder. This dose, 0.01dpa, was enough to induce significant degradation in thermal diffusivity. Thermal diffusivity was measured by laser flash method in the previous work, and that showed about 20%, 40%, 30%, 75% degradation for α-Al_2O_3, AlN, β-Si_3N_4 and β-SiC respectively.

Positron annihilation lifetime was also measured using conventional γ-γ fast coincidence method in Radiation Laboratory, Uji. The irradiated specimen was ϕ10x2mm disk, but the number of the specimen was only one for each material. Usually, γ-γ coincidence PAL method requires two peaces of specimens to put a positron source between specimens. In this work, we used one peace of non-irradiated specimen at the other side of the irradiated specimen. Positron source was 0.5MBq ^{22}Na sealed by Ti foil, and the active diameter was 1mm.

The obtained PAL spectrum was analyzed with PALSfit program [4], with resolution FWHM about 300 ps. In analyze of the spectrum, a source component that represents annihilation in the Ti foil was not resolved, and only two or three component was guessed in the analysis.

RESULTS:

After the spectrum analysis, average positron lifetime $\langle\tau\rangle$ was obtained as $\langle\tau\rangle = \tau_1 I_1 + \tau_2 I_2$, where τ_i are the analyzed positron lifetimes and I_i are the intensities for the components. The average lifetime $\langle\tau\rangle$ of electron irradiated α-Al_2O_3 indicated significant increment same as neutron irradiated specimens. On the other hand, AlN and β−Si_3N_4 showed distorted spectrum because of radioactivation, so the measurement was planed in the next year (the $t_{1/2}$ of the radioactivated nuclide was 107day). In the case of β-SiC showed almost no change in lifetime same as neutron irradiated specimen.

At last, average positron lifetime was compared with thermal diffusivity. Fig.1 shows the result in α-Al_2O_3 irradiated electron and also neutron. α-Al_2O_3 showed most close correlation between thermal diffusivity and $\langle\tau\rangle$. On the other hand, the thermal diffusivity of unirradiated specimen was no so high, while unirradiated AlN showed very high thermal diffusivity that make easy to evaluate the difference after an irradiation.

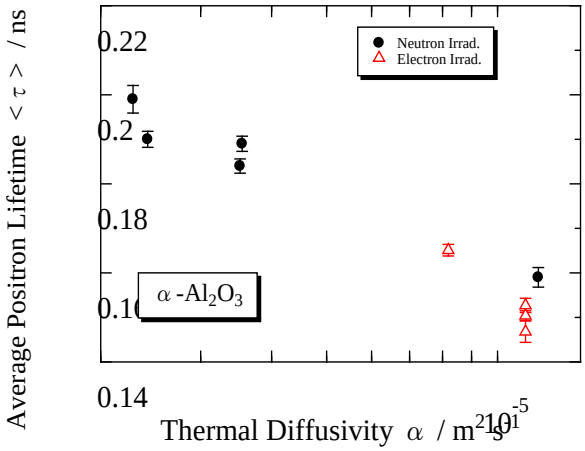

Fig. 1. Change of average positron lifetime in electron and neutron irradiated α-Al_2O_3 compared with thermal diffusivity. The origin of specimen for electron irradiation and neutron irradiation was different, and thermal diffusivity and $\langle\tau\rangle$ was different even in the unirradiated specimen.

REFERENCES:

[1] M. Akiyoshi *et al.*, J. Nucl. Mater., **367-370** (2007) 1023.
[2] M. Akiyoshi *et al.*, Fus. Eng. Design., **81** (2006) 321.
[3] M. Akiyoshi *et al.*, J. Nucl. Mater., **307-311** (2002) 1305.
[4] P. Kirkegaard, J.V. Olsen, M. Eldrup, and N.J. Pedersen, Riso DTU, Riso-R-1652, 2009.

採択課題番号 21P1-5　照射セラミックスの熱拡散率及び陽電子消滅法による欠陥評価　プロジェクト
（京大・工）秋吉 優史、高木 郁二（京大・原子炉）義家 敏正、徐 虬、佐藤 紘一

PR1-6 Vacancy-Type Defects in Cu-Cr-Zr Alloy Induced by 28 MeV Electron Irradiation at 77K Studied by Positron Annihilation

Y. Nagai[1], T. Toyama[1], M. Hatakeyama[1], A. Kuramoto[1], H. Takamizawa[1], T. Yoshiie[2] and Q. Xu[2]

[1]*Institute for Materials Research, Tohoku University*
[2]*Research Reactor Institute, Kyoto University*

INTRODUCTION: Cu-Cr-Zr alloy is one of the candidate materials for the heat sink of the International Termonuclear Experimental Reactor (ITER) divertor, because of high strength and high conductivity of the alloy. These excellent properties are obtained by microscopic structures: particle-dispersion strengthening with Cr-rich precipitates and the very low solubility of Cr and Zr in the Cu matrix. We have recently suggested that vacancy-type defects are associated with Cr atoms around the precipitate-matrix interfaces [1]. The purpose of this study is to make clear the difference between the interface defects and irradiation-induced defects using positron annihilation techniques.

EXPERIMENTAL: The chemical composition of the studied material is Cu-0.78Cr-0.13Zr-0.003Si-0.008Fe in weight percent. The Cu-Cr-Zr samples were solution annealed at 960 °C for 3h followed by water-quenching, then aged at 460 °C for 3h and 600 °C for 1h. The details of the heat treatment are described in refs. [1, 2]. Cr-rich precipitates of ~10 nm in diameter formed and dispersed homogeneously before irradiation. The samples were irradiated at 77K by 28MeV electrons to a fluence of 1×10^{19} e/cm^2 using the KUR-LINAC. Pure Cu was also irradiated as a reference. The samples were set to a sample chamber for positron lifetime and coincidence Doppler broadening (CDB) apparatus without temperature rise. The measurements were performed at ~80K.

RESULTS & DISCUSSION: Table 1 shows the positron lifetime measurements of pure Cu and Cu-Cr-Zr. In pure Cu, the average lifetime (τ_{av}) increased after irradiation due to the irradiation-induced defects. In Cu-Cr-Zr, τ_{av} is longer than that of bulk Cu even in the unirradiated state because of the positron trapping at V_1 and/or dislocations associated with the Cr-rich precipitates induced by the heat treatment [1]. After irradiation, small increase of τ_{av} was observed. This shows that positron annihilates also at the irradiation-induced defects.

Table 1: Positron lifetime measurements of electron-irradiated pure Cu and Cu-Cr-Zr.

		τ_{av}	τ_1	τ_2	I_2
Pure Cu	Unirrad.	110.0±0.2			
	As-irrad.	175.4±0.2	75.1±0.4	186.5±2.5	85.6±2.5
Cu-Cr-Zr	Unirrad.	164.3±0.2	48.0±1.2	179.0±2.1	88.0±0.7
	As-irrad.	168.8±0.2	65.0±1.2	181.1±2.3	89.0±1.2

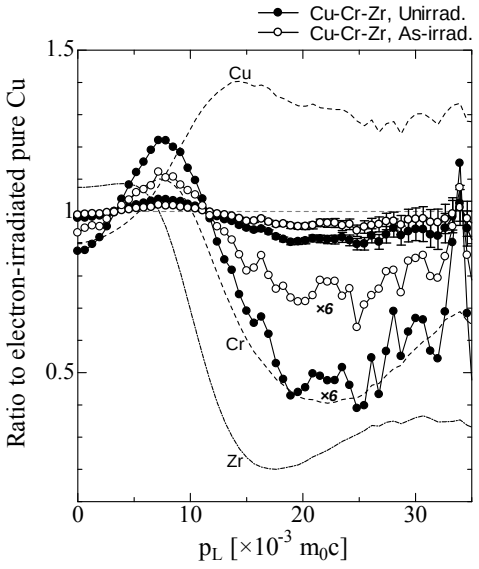

Fig. 1. CDB spectra of the Cu-Cr-Zr alloys as ratio to the electron-irradiated pure Cu. CDB spectra of the well-annealed pure Cu, Cr and Zr are also shown as references.

Figure 1 shows CDB spectra of the unirradiated and the irradiated Cu-Cr-Zr as ratio to the electron-irradiated pure Cu together with those of the well-annealed pure Cu, Cr and Zr as references. In the unirradiated Cu-Cr-Zr, a broad valley centered around 20×10^{-3} m_0c is observed. The spectrum multiplied by a factor of 6 is found to be very close to that of pure Cr, showing that about 1/6 of positrons annihilate with Cr electrons and the remaining 5/6 of positrons annihilate with Cu electrons. This suggests that the vacancy-type defects exist both in the interfaces between Cr-rich precipitates and matrix and in Cu matrix [1]. After irradiation, the broad valley was markedly dehanced and the CDB spectrum was close to that of the electron-irradiated pure Cu. This shows that positron annihilation fraction with Cr electrons decreased after irradiation, suggesting that Cr-free defects are induced in Cu matrix by electron irradiation at low temperature.

The irradiation effect on morphologies of the Cr-rich precipitates will be investigated by three-dimensional atom probe and transmission electron microscope in a further study.

[1] M. Hatakeyama et al., J. Nucl. Mater., **386** (2009) 852.
[2] M. Hatakeyama et al., Mater. Trans., **49**(3) (2008) 518.

採択課題番号 21P1-6　　原子力材料および半導体の低温照射効果　　プロジェクト
（東北大・金研）永井康介、外山健、畠山賢彦、蔵本明、高見沢悠
（京大・原子炉実験所）義家敏正、徐　虬

PR1-7 Defects Study for Bulk Glassy Alloys Damaged by Electron Irradiation

F. Hori, Y. Fukumoto, A. Ishii, S. Mineno, A. Iwase
Q. Xu[1] and T. Yoshiie[1]

Dept. of Mater. Sci., Osaka Prefecture University
[1]*Research Reactor Institute, Kyoto University*

INTRODUCTION: The bulk metallic glasses (BMGs) are expected to be useful for various applications due to their superior mechanical properties, hardness, strength, corrosion resistance and micro-formability [1-3]. The free volume in bulk metallic glass alloys has a significant effect on atomic relaxation and crystallization processes, although a detailed atomic configurations and their motion around free volume site has not been clarified yet. Also the free volume has significant effects on various properties. Nevertheless, the radiation effect of high energetic particle irradiations on the structure and various properties change for bulk metallic glass. Positron annihilation is a unique technique and sensitive to detect the atomic size open volume in materials. Then we examined free volume change for ternary Zr-Cu-Al metallic glass after energetic particles irradiations by positron annihilation lifetime and coincidence Doppler broadening techniques.

EXPERIMENTS: A bulk size of $Zr_{50}Cu_{40}Al_{10}$ metallic glass with 8 mm in diameter and 60 mm in length was prepared by a tilt casting technique. For positron annihilation measurements, alloy sample was cut into the size of about 0.5 mm thickness. Electron irradiation with total doses from $4.0x10^{17}$ to $5.0x10^{18}$ e/cm^2 was performed for this alloy at 100 K by LINAC at Research Reactor Institute, Kyoto University. Irradiated samples were examined by X-ray diffraction, positron annihilation lifetime and coincidence Doppler broadening (CDB) measurements at room temperature

RESULTS: X-ray diffraction results show that crystallization dose not occurs by electron irradiation as shown in figure 1. On the other hand, positron lifetimes of 166 psec for bulk ZrCuAl metallic glass and greater value than bulk for electron irradiated samples have already reported. Fig. 2 shows the CDB ratio spectra (ratio to that of pure Al) obtained for before and after electron irradiation. There is no significant change in the CDB ratio spectra before and after electron irradiation. This means that electron irradiation makes increasing the size of free volume without atomic reconstruction around free volume. Recent years, it was reported the crystallization and local structure relaxation by ion irradiation with various energies to Zr based BMGs [4,5]. We suggested that the damage structure in bulk metallic glasses by irradiation is strongly affected by the irradiation species and irradiation energy.

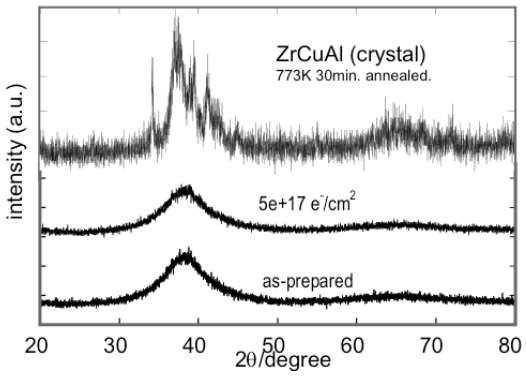

Fig. 1. XRD profiles for before and after electron irradiated ZrCuAl bulk metallic glass. Also shows for crystallized one.

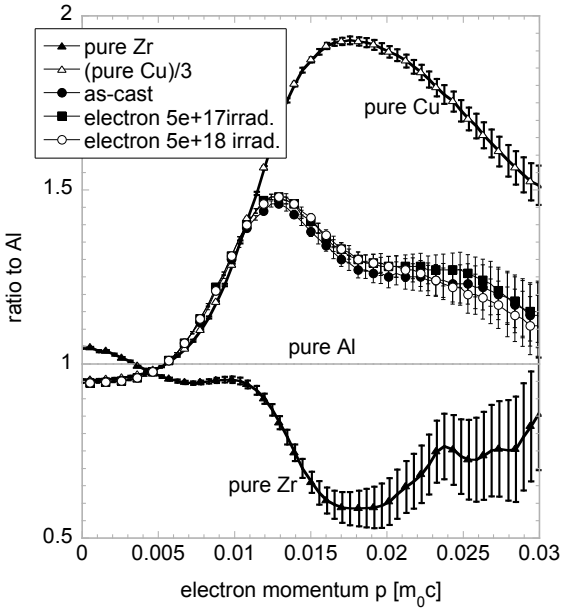

Fig. 2. Coincidence Doppler broadening ratio spectra for before and after 30MeV electron irradiated ZrCuAl bulk metallic glass.

REFERENCES

[1] Inoue A 2000 Acta. Mater. **48** 279.
[2] Löffler J F 2003 Intermetallics **11** 529.
[3] Johnson W L 2002 JOM. **54** 40.
[4] Nagata S 2009 Nucl. Inst. Meth. B **267** 1514.
[5] Fukumoto Y 2010 J. Phys. C to be published.

採択課題番号 21P1-7　　金属合金における照射効果の研究　　プロジェクト
（阪府大・工）堀史説、福本由佳、石井顕人、峯野慎也、岩瀬彰宏
（京大・原子炉）徐虬、義家敏正

PR1-8 Microstructure of Neutron Irradiated Vanadium Alloys in a Liquid Sodium Environment

K. Fukumoto[1], M. Iwasaki[2] and Q. Xu[3]
[1] *RINE, Univ. of Fukui*
[2] *Graduate school of Eng., Univ. of Fukui*
[3] *Research Reactor Institute, Kyoto University*

INTRODUCTION: Vanadium alloys are candidate materials for blanket structural materials in fusion reactors, but knowledge about their mechanical properties at high temperatures during neutron irradiation is limited and there are uncertainties, such as the interstitial impurity content of the specimens that may influence the results. In this study, tensile tests and TEM measurements were carried out on V-4Cr-xTi alloys after aging by heat treatment. The aging behavior of the dynamic strain for the V-4Cr-4Ti alloys was measured and was compared with that of other V-4Cr-xTi alloys. The purpose of this study is to make clear the thermal process of Ti(OCN) precipitation and the distribution of interstitial impurities in V-4Cr-4Ti alloys during heat treatment.

EXPERIMENTS: SSJ tensile specimens of V-4Cr-xTi(x=0.1, 0.3, 1, 3 and 4) were used. The impurity levels are 500-600 wppm for O and <20 wppm for N and C. Table 1 shows a list of interstitial impurity levels for the alloys. The annealing conditions are 1000°C for 2 hr. The specimens were wrapped with Ta and Zr foils and enclosed in a quartz tube in vacuum. The thermal aging treatment was performed by placing the sealed quartz tubes in a Muffle furnace at a temperature between 600 and 800 ˚C for 100 or 1000 hr. After the heat treatment, tensile tests were performed at a strain rate of 6.67×10^{-4}/s at room temperature and 500˚C in a vacuum. TEM samples were punched from non-deformed areas of the tested specimens.

RESULTS: When test temperature in the tensile tests was increased, the yield stress decreased for all annealed specimens. When the proportion of titanium in the V-4Cr-xTi alloys increased, the yield stress and ultimate tensile stress (UTS) increased and the serration behavior in the stress–strain curve was more pronounced. In particular, the specimen aged at 600°C for 100 hr showed a large degree of hardening, but the ones aged at 800°C for 100 hr showed a smaller degree of hardening or even softening. With the addition of titanium to the V-4Cr-xTi alloys the yield stress vs. test temperature was reduced but the change of yield stress vs. ageing temperature was increased.

In this study, a test temperature of 500°C was selected because the amplitude of the serration behavior at 500°C was larger than that at other test temperatures. A continuous yield drop of the flow stress, known as type II serration, can be seen in V-4Cr-0.1Ti and -0.3Ti alloys aged at 600°C for 100 hr. On the other hand, continuous yield drops around the flow stress did not appear and discontinuous, large yield drops after UTS appeared in V-4Cr-1Ti and -3Ti alloys. After ageing at 800°C, type II serration behavior occurred in V-4Cr-0.1Ti and -0.3Ti alloys, but the stress amplitudes of the serration behavior were smaller than for those samples aged at 600°C. In V-4Cr-3Ti alloys, serration behavior with a large amplitude of serration occurred. The dependence of serration amplitude behavior in V-4Cr-xTi alloys as a function of titanium addition was measured for the jerky-flow from the yield point to the UTS point on stress-strain curve. This test was performed at 500°C for samples following all heat treatment conditions.

Figure 1 shows the ageing time dependence of the mean serration amplitude on the stress–strain curve for V-4Cr-1Ti alloys aged at 600°C and 800°C. The 10 MPa serration amplitude for the as-annealed specimen disappeared completely after heat treatment ageing at 600°C for 100 hr and 1000 hr. For the sample aged at 800°C, the serration amplitude decreased significantly after 100 hr of ageing and the amplitude was suppressed completely after 1000 hr ageing. From these results, we conclude that large microstructural changes may occur during the initial period of the ageing process at 600°C and 800°C, affecting the dynamic strain .

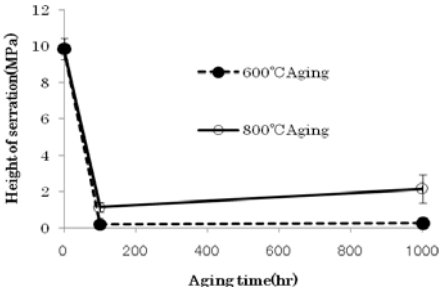

Fig. 1. The mean serration amplitude in the stress – strain curve vs. ageing time for V-4Cr-1Ti aged at 600°C and 800°C.

採択課題番号21P1-8　Li 雰囲気中性子照射したバナジウム合金の微細組織構造に関する研究　プロジェクト

（福井大院工）福元謙一、岩崎将大（京大・原子炉）徐　虬

PR1-9

Damage Evolution in Neutron-Irradiated Metals During Neutron Irradiation at Elevated Temperatures

I. Mukouda, K. Yamakawa[1], T. Yoshiie[2] and Q. Xu[2]

Hiroshima International University,
[1]Faculty of Engineering, Ehime University
[2]Research Reactor Institute, Kyoto University

INTRODUCTION: A structural ordering of atoms in Au_3Cu alloys has been investigated by the electrical resistivity measurements. The measuring temperature dependence of isothermal resistance curve has been investigated theoretically and experimentally during precipitating.

In the previous report we found that the isothermal annealing time at the resistance maximum measured at liquid nitrogen temperature was longer than it measured at the annealing temperature (higher temperature)[1].

In the present experiment the electrical resistances of the Au_3Cu alloy are measured at more numbers of temperature during ordering and discussed comparing with theoretical results.

EXPERIMENTS: The electrical resistance was measured during the annealing at the high temperature and measured at iced water, liquid nitrogen and liquid helium temperature. After each annealing the tube was quickly pulled out from the furnace and put into the iced water. Then the tube was quenched into liquid nitrogen and liquid helium in order. Therefore, the resistance is measured at the same structural condition as it at the high temperature. The resistance measurement was done by standard four probe method.

RESULTS: After the quenching from T_Q-400°C the isothermal resistance curves measured at various temperatures are shown in Fig.1. The annealing time at the resistance maximum decreases, in order, with the measuring temperature (T_M) decrease. The curves are shifted in y-axis to show the difference of annealing time between the maximums more clearly. The amounts of shift of the curves are shown in the figure, respectively. After the quenching, similar curves are shown in Fig.2 for different annealing temperatures. Each curve in Fig.2 shows the resistance maximum and similar behavior of the time position of maximum, though the quenching and annealing temperature are different from those in Fig.1. The curves annealed at the same temperature (150°C) are able to compare with each other for different T_Q from Figs.1 and 2. As expected, each curve at various T_M shows the resistance maximum at shorter annealing time in the case of higher T_Q.

The isothermal resistance curves are shifted to shorter time by quenching from higher temperature. These are caused by vacancies in abundance introduced by quenching treatment because the ordering would be caused by vacancy diffusion.

Hillel's group and Rossitor's group proposed the mechanisms to explain the maximum on resistivity curve[2]. Their results are summarized as follows. If the precipitates are spherical, the position of the resistance maximum dose not shift with increase of the measuring temperature, If the precipitates are not spherical, the position shifts to long annealing time direction with increase of the measuring temperature.

In the present experiments as shown in Figs. 1 and 2, the isothermal annealing time at the resistance maximum shifts to longer annealing time with increase of the measuring temperature. Therefore, it is concluded that, during the ordering on Au_3Cu alloy, the ordered domains are not spherical but platelet.

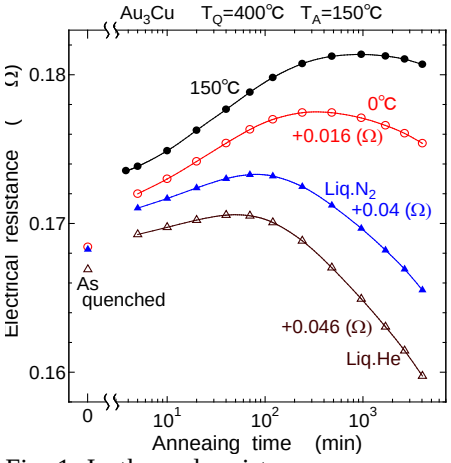

Fig. 1. Isothermal resistance curves measured at various temperatures.

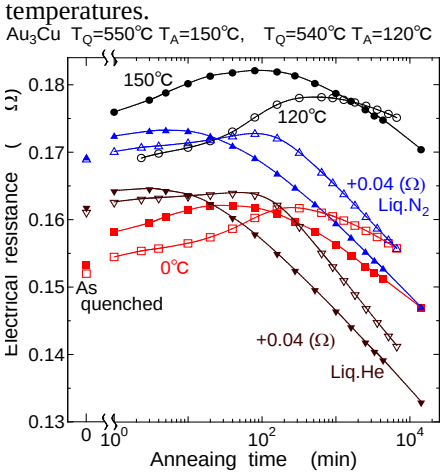

Fig. 2. Isothermal resistance curves measured at various temperatures.

REFERENCES:

[1] K. Yamakawa, Y. Yoshida, J. Alloys Comp. in print (2010).
[2] A.J. Hillel, P.L. Rossitor, Phil. Mag. B**44**(1981) 383.

採択課題番号 21P1-9　高温での中性子照射金属中の点欠陥集合体動的挙動と損傷組織発達過程　プロジェクト

（広島国際大学）向田一郎、（愛媛大）山川浩二、（京大原子炉）義家敏正、徐　虬

PR1-10 Effects of Thermal Aging on Positron Annihilation Behaviors of ODS and Non-ODS Ferritic Steels

R. Kasada[1], S.H. Noh[2], J.H. Lee[1], A. Kimura[1], K. Sato[3], Q. Xu[3] and T. Yoshiie[3]

[1]*Institute of Advanced Energy, Kyoto University*
[2]*Graduate School of Energy Science, Kyoto University*
[3]*Research Reactor Institute, Kyoto University*

INTRODUCTION: Oxide dispersion strengthened (ODS) ferritic steels containing nano-oxide particles are one of the attractive materials for next generation nuclear fission systems as well as for fusion reactors because of the excellent high-temperature strength and irradiation resistance [1]. Furthermore, the high-Cr (>15wt%) ODS ferritic steels developed by the SUPER-ODS project conducted by Kyoto University has superior corrosion resistance against super-critical water and liquid lead bismuth eutectic alloy [2]. However, these high-Cr steels will suffer from thermal aging embrittlement, which is well-known 475 °C embrittlement, due to phase separation of Fe and Cr. Here, we are applying positron annihilation spectrometry to detect the phase separation in the high-Cr ODS steels as well as in the non-ODS ferritic steel. Positron trapping behavior in the ODS alloys is also discussed in order to use the positron annihilation spectrometry.

EXPERIMENTAL PROCEDURE: Materials used in the present study is ODS ferritic steels which are named K1 (Fe-19Cr-0.5W-0.3Ti-0.3Y_2O_3) and K4(Fe-19Cr-4Al -2W-0.3Ti-0.3Y_2O_3), and non-ODS commercial ferritic steel SUS430 (Fe-16Cr). Thermal aging treatment on these materials was carried out at 400 °C up to 2400 h. Positron annihilation spectrometry (PAS), including coincidence Doppler broadening (CDB) technique and lifetime measurement, were performed in the KURRI.

RESULTS AND DISCUSSIONS: Regarding mechanical property investigations and transmission electron microscopy on the ODS steels and SUS430, thermal aging embrittlement and Cr-rich phase formation was confirmed. Results of positron annihilation lifetime spectrometry and CDB spectrometry on the ODS steels and SUS430 are summarized in Table 1 and Fig. 1, respectively. The lifetime and CDB ratio in the SUS430 showed no significant change before and after the thermal aging. This result suggests that positron trapping behavior is not affected by the Cr-rich phase formation in the thermally-aged Fe-16Cr steel. The lower positron affinity of Cr than Fe well explains the present results [3]. On the other hand, the ODS steels indicated slight change in the CDB ratio curves but no meaningful change in the lifetime. Further experiments and theoretical approach are needed to clarify the state of positron trapping in the ODS steels.

Table 1. Results of positron lifetime on the ODS steels and SUS430 before and after thermal aging at 400 °C up to 2400 h.

試料	τ_m	τ_1	I_1	τ_2	I_2	τ_3	I_3
SUS430 As-received	109±1						
SUS430 400C, 2400h	112±1						
ODS-K1 As-received	204±1	132±4	39±3	242±3	61±3		
ODS-K1 400C, 2400h	194±1	117±3	41±2	240±2	59±3		
ODS-K4 As-received	205±1	115±2	44±1	264±2	56±1		
ODS-K4 400C, 2400h	203±1	48±4	18±1	182±7	60±3	326±14	22±4

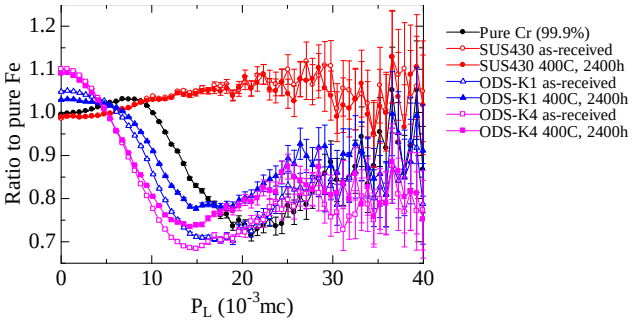

Fig. 1. Positron CDB ratio-curves obtained for the ODS steels and SUS430 before and after thermal aging at 400 °C up to 2400 h.

REFERENCES:

[1] K. Yutani, H. Kishimoto, R. Kasada, A. Kimura, J. Nucl., Mater., 367-370 (2007) 423.
[2] A. Kimura, R. Kasada, N. Iwata, H. Kishimoto, C. Zhang, P. Dou, J. Isselin, N. Muthkumar, J. Lee, T. Okuda, M. Inoue, S. Ukai, S. Ohnuki, T. Fujisawa, F. Abe, Proceedings of ICAPP'09, 2009, 9220.
[3] M J Puska, P Lanki and R M Nieminen, J. Phys. Condens. Matter 1 (1989) 6081.

採択課題番号 21P1-10　　酸化物分散強化鋼のナノ構造に及ぼす熱時効効果及び照射効果　　プロジェクト

（京大・エネ研）木村　晃彦、笠田　竜太　（京大原子炉）義家　敏正、徐　虬、佐藤　紘一
（京大院・エネ科）Lee Jaehoon、Noh Sanghoon

PR1-11

Interaction Between Radiation Defects and Hydrogen Studied by Positron Annihilation Spectroscopy

H. Tsuchida, H. Tanaka[1], A. Itoh[1], T. Yoshiie[2] and Q. Xu[2]

Quantum Science and Engineering Center, Graduate School of Engineering, Kyoto University
[1]Depertment of Nuclear Engineering, Kyoto University
[2]Research Reactor Institute, Kyoto University

INTRODUCTION: Hydrogen effect on void nucleation is important subjects in research of nuclear reactor materials. Hydrogen is known to be produced in materials irradiated with a fast neutron via the nuclear reaction (n, p). The hydrogen is trapped in radiation defects [1]. This induces significant mechanical property degradation. At present many studies have been carried out on interaction of hydrogen with vacancy defects. However, hydrogen effect on the initial stage of growth of vacancy defects, especially micro-void formation process, is not fully understood.

In this work, we studied vacancy defects in stainless-steel induced by high-flux hydrogen irradiation by two kinds of positron annihilation spectroscopy: positron annihilation lifetime (PALS) and coincidence Doppler broadening (CDB) spectroscopy.

EXPERIMENTS: Samples were two types of stainless-steel of 304 and 316L, they were annealed at 1473 K for 1 h in vacuum. The samples were irradiated with hydrogen ions at two different incident energies of 3.0 and 4.0 MeV. Total fluence was about 1×10^{17} ions/cm^2, which corresponds to about 3×10^{-3} dpa estimated from TRIM code. Irradiation was carried out under low temperature conditions. Sample temperatures during irradiation were kept below 240 K to avoid diffusion of implanted hydrogen due to beam-heating effect.

Radiation defects in the sample after irradiation were measured by using the apparatus of positron annihilation spectroscopy at KURRI.

RESULTS: Results of the PALS were listed in Table 1. For both SUS 304 and 316L, values of the long lifetime were about 200 ps and the corresponding vacancy type was tri-vacancies. These results are the same for incident energies of 3.0 and 4.0 MeV. Figure 1 shows results of the CDB spectroscopy. Results show that for irradiated sample the value of ratio to pure Fe significantly exceeds 1 below 5×10^{-3} mc (at the low electron- momentum region), indicating existence of vacancy defects. Detection of hydrogen cannot be seen from variation of the CDB curves obtained in this work. .

(a) SUS304

Incident energy [MeV]	Mean lifetime [ps]	Two component analysis	
		Lifetime [ps]	Long lifetime Intensity [%]
3.0	182.6	100.6 (short) 205.5 (long)	74
4.0	188.7	102.9 (short) 205.3 (long)	80

(b) SUS 316L

Incident energy [MeV]	Mean lifetime [ps]	Two component analysis	
		Lifetime [ps]	Long lifetime Intensity [%]
3.0	177.1	110.5 (short) 203.5 (long)	68
4.0	184.7	92.2 (short) 195.2(long)	87

Table 1. Experimental results of positron lifetime and its intensity for samples of (a) SUS304 and (b) SUS316L.

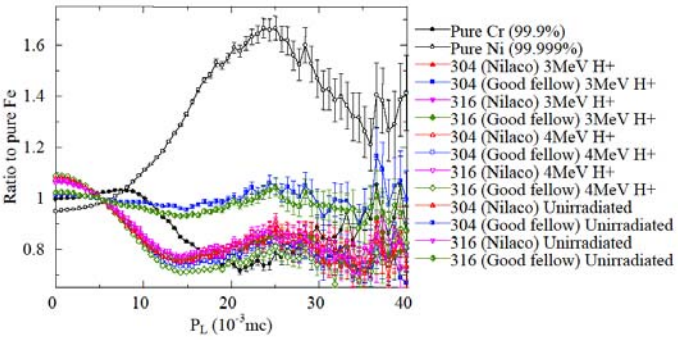

Fig. 1. Experimental results of CDB curve normalized to that of pure Fe as a function of momentum of electrons.

REFERENCES:

[1] C. He *et. al*., Philosopical Magazine., **89** (2009) 1183.

採択課題番号 21P1-11　陽電子消滅法によるプロトン照射した金属材の照射欠陥周辺の水素検出に関する研究　プロジェクト

（京大院工）土田秀次、田中　拓、伊藤秋男（京大・原子炉）義家敏正、徐　虬

PR1-12 Austenitic Stainless Steel Irradiated with High-Energy Particle at High Temperature

K. Sato, X.Z. Cao, Q. Xu and T. Yoshiie

Research Reactor Institute, Kyoto University

INTRODUCTION: Austenitic stainless steel is an important nuclear material, but it is vulnerable to void swelling during prolonged neutron irradiation. Such swelling in neutron-irradiated steel has been studied extensively for many years. Experimental and theoretical analyses revealed the importance of an incubation dose, which is a transient dose required before steady state void growth occurs [1, 2]. The duration of the incubation period determines the lifetime of the steel. However, experimental results for void swelling in austenitic stainless steel have been limited only to the high dose regime. As the main method to study defect structures has been transmission electron microscopy, it was impossible to detect not only mono-vacancies but also small microvoids during the incubation period. Therefore, there is little information about the behavior of vacancies during this period. Positron annihilation spectroscopy makes it possible to detect vacancy clusters, even single vacancies. There have been, however, only few studies of damage structures in austenitic stainless steel by using it.

In this study, point defect processes occurring during the incubation period of austenitic stainless steel were studied using positron annihilation lifetime measurements, which enable us to detect the existence of mono-vacancies.

EXPERIMENTS: The samples used in this study were listed in Table 1. Electron irradiation was performed by an electron linear accelerator of Kyoto University with an accelerating voltage of 30 MV. Irradiation temperature was room temperature (RT) and 573K. Irradiation dose was 1.2 x 10^{-2}dpa and 1.5 x 10^{-2}dpa, respectively. After introduction of defects by irradiation, positron annihilation lifetimes were measured at room temperature using a conventional fast-fast spectrometer with a time resolution of 190 ps (full width at half maximum) and each spectrum was accumulated to a total of 1×10^6 counts. Positron annihilation lifetimes of defects in commercial austenitic stainless steels have not yet been calculated. Only the lifetime of a model alloy of austenitic stainless steel, Fe-14Cr-13Ni, was calculated based on a first principles approach [3], and the lifetimes were found to be 106 and 183 ps for the matrix and mono-vacancies, respectively. These values are almost the same as those for Ni [4]. For this reason we used the lifetime of Ni for the estimation of defect clusters such as microvoids, stacking fault tetrahedra and dislocations [5].

RESULTS: In samples irradiated at RT, single, di- or tri-vacancies were formed. In all samples irradiated at 573K, mean lifetime was shorter than that of samples irradiated at RT. This is because point defects migrate easily, and frequency of mutual annihilation between vacancies and interstitials increase. In sample A, B and C irradiated at 573K, vacancy clusters, which were composed of four or five vacancies, grew compared with those irradiated at RT. In sample Ni and D, stacking fault tetrahedra were detected, and in sample E, F, J and G, vacancy clusters were not detected. In RT irradiation, vacancies have short-range migration, and we cannot detect the solute atom effect. On the other hand, we can detect it at 573K irradiation. Positron annihilation spectroscopy is very powerful tool to obtain vacancy cluster growth process in the incubation period of void growth of austenitic stainless steel.

Table 1. Chemical composition of samples used in this study.

Sample number	Chemical composition
Ni	Pure Ni (99.99%)
A	Fe-16.13Cr-16.96Ni
B	Fe-15.39Cr-15.92Ni-1.89Mn-2.68Mo
C	Fe-15.27Cr-15.8Ni-1.88Mn-2.66Mo-0.53Si
D	Fe-15.27Cr-15.8Ni-1.88Mn-2.66Mo-0.53Si-0.24Ti
E	SUS316L
F	SUS316
J	Fe-15.27Cr-15.8Ni-1.88Mn-2.66Mo-0.53Si-0.24Ti-0.055C-0.024P
G	SUS304

Table 2. Positron annihilation lifetime of stainless steels and their model alloys irradiated with electrons at room temperature (Irradiation dose: 1.2 x 10^{-2}dpa).

Sample number	τ_{av} (ps)	τ_1 (ps)	τ_2 (ps)	I_2 (%)
Ni	156±1	135±6	220±19	19±7
A	183±1	140±11	218±10	47±10
B	180±1	134±15	205±10	55±13
C	180±1	123±13	184±2	67±4
D	183±1	140±9	220±9	46±8
E	181±1	142±13	211±12	49±14
F	180±1	124±15	202±7	62±10
J	179±1	116±14	196±5	69±7
G	184±1	158±9	237±19	28±12

Table 3. Positron annihilation lifetime of stainless steels and their model alloys irradiated with electrons at 573K (Irradiation dose: 1.5 x 10^{-2}dpa).

Sample number	τ_{av} (ps)	τ_1 (ps)	τ_2 (ps)	I_2 (%)
Ni	118 ± 1	84 ± 3	151 ± 5	43 ± 5
A	133 ± 1	84 ± 1	246 ± 3	27 ± 1
B	144 ± 1	79 ± 1	256 ± 2	32 ± 1
C	111 ± 1	96 ± 1	227 ± 11	9 ± 1
D	108 ± 1	86 ± 5	135 ± 10	36 ± 13
E	106 ± 1			
F	106 ± 1			
J	107 ± 1			
G	106 ± 1			

REFERENCES:

[1] F. A. Garner, Nuclear Materials, vol. **10A** (1994) 419.
[2] L. K. Mansur *et al.*, J. Nucl. Mater., **119** (1983) 1.
[3] T. Yoshiie *et al.*, Phys. Stat. Sol. C (2010) Accepted.
[4] B.L. Shivachev *et al.*, J. Nucl. Mater. **306** (2002) 105.
[5] E. Kuramoto *et al.*, Comput. Mater. Sci. **14** (1999) 28.

採択課題番号 21P1-12　　金属における電子線による照射効果　　プロジェクト
（京大・原子炉）佐藤紘一、曹興忠、徐　虬、義家敏正